Study and modeling of finite rate chemistry effects in turbulent non-premixed flames

By Luc Vervisch

1. Background and objectives

The development of numerical models that reflect some of the most important features of turbulent reacting flows requires information about the behavior of key quantities in well defined combustion regimes. In turbulent flames, the coupling between turbulent and chemical processes is so strong that it is extremely difficult to isolate the role played by one individual physical phenomenon. Direct numerical simulation (hereafter DNS) allows us to study in detail the turbulence-chemistry interaction in some restricted but completely defined situations. Globally, non-premixed flames are controlled by two limiting regimes: the fast chemistry case, where the turbulent flame can be pictured as a random distribution of local chemical equilibrium problems; and the slow chemistry case, where the chemistry integrates in time the turbulent fluctuations. The Damköhler number, ratio of a mechanical time scale to a chemical time scale, is used to distinguish between these regimes. Today most of the industrial computer codes are able to perform predictions in the hypothesis of local equilibrium chemistry using a presumed shape for the probability density function (hereafter pdf) of the conserved scalar (Couplan *et al.* 1987, Viollet *et al.* 1990). However, the finite rate chemistry situation is of great interest because industrial burners usually generate regimes in which, at some points, the flame is undergoing local extinction or at least non-equilibrium situations. Moreover, this variety of situations strongly influences the production of pollutants (Masri *et al.* 1988).

To quantify finite rate chemistry effect, the interaction between a non-premixed flame and a free decaying turbulence is studied using DNS. The attention is focused on the dynamic of extinction, and an attempt is made to quantify the effect of the reaction on the small scale mixing process (section 2). The unequal diffusivity effect is also addressed (section 3). Finally, a simple turbulent combustion model based on the DNS observations and tractable in real flow configurations is proposed (section 4).

2. Finite rate chemistry effects in turbulent non-premixed flames

Three-dimensional direct numerical simulations of non-premixed flames have been carried out using a high-order finite difference code (Trouvé, 1991). Reacting flows are simulated resolving all of the scales of the turbulent motion, including effects due to variations in density and viscosity (Poinsot 1989, Poinsot *et al.* 1991). The chemistry is represented through a single-step reaction $A + B \rightarrow P$ or a two-step process $A+B \rightarrow I$, $A+I \rightarrow P$. The parameters of the Arrhenius-type reaction rate model chosen for the single-step simulations are close to that of global Methane-Air

combustion. The second mechanism is an attempt to study the effect of radical-like species in turbulent non-premixed flames. The second step ($A + I \rightarrow P$) proceeds with an activation energy four times smaller and an enthalpy of reaction five times larger compared to the first step.

The turbulent simulations are initialized by a well characterized one-dimensional, planar, laminar non-premixed flame which has been previously generated by the code (Chen *et al.* 1992). A prescribed turbulent field interacting with the initially laminar flame is then allowed to decay. The value of the initial Taylor Reynolds number is the order of fifty, a value relevant for some jet flames (Dibble *et al.* 1986; Magre *et al.* 1988), where the Reynolds number based on the velocity profile half-width increases from fifty to eighty along the jet axis.

The Damköhler number, defined as the ratio of the turbulent eddy turnover time to a chemical time based on the heat release of the initial laminar flame, is varied over a range corresponding to fast and slow chemistry in order to study the effect of finite-rate chemistry on flame structure. The flame thickness is such that the flame-flow interactions are limited to a range of reactive and turbulent scales of the same order of magnitude.

2.1 One-step chemistry model

It is observed in the case of intermediate value of the Damköhler number (regime ranging between slow and fast chemistry) that points exist which are influenced by the fully burning and extinguished locations. In the plane (Y_A, Z) defined by species A mass fraction and the mixture fraction (a conserved scalar, Z), these points are located between the lower bound on the species concentration distribution (equilibrium line, stoichiometric value, $Z_{St} = 0.5$) and the upper bound (pure mixing), Figure 1. This is representative of a turbulence-induced mixing influencing both full burning and frozen flow points, and it corresponds to a transient response. Indeed, in the (Y_A, Z) space, the concentration of a fluid particle is governed by (Lagrangian frame) :

$$\frac{dY_A}{dZ} = \frac{\frac{\partial}{\partial x_i}\left(\rho \mathcal{D}_A \frac{\partial Y_A}{\partial x_i}\right) + \dot{w}_A}{\frac{\partial}{\partial x_i}\left(\rho \mathcal{D} \frac{\partial Z}{\partial x_i}\right)}. \tag{1}$$

According to this equation, depending on the time scale involved in the small scale diffusion process (enhanced by the turbulence) and in the reactive phenomenon ($\dot{w}_A$), the concentration of the fluid particle in the plane (Y_A, Z) could reach all the values in the domain that lies between the pure mixing line and the fast chemistry line. The transient response is due to the effect of diffusion at small scale which is affected by the turbulence modifying the instantaneous species profile and, therefore, the reaction rate. This transient response is representative of the finite-rate chemistry effect.

It has been verified (Chen *et al.* 1992) that in the databases, the stoichiometric surface and the location of peak reaction zone coincide, and also that contours of Z are parallel within the reaction zone. The mixture fraction dissipation rate χ

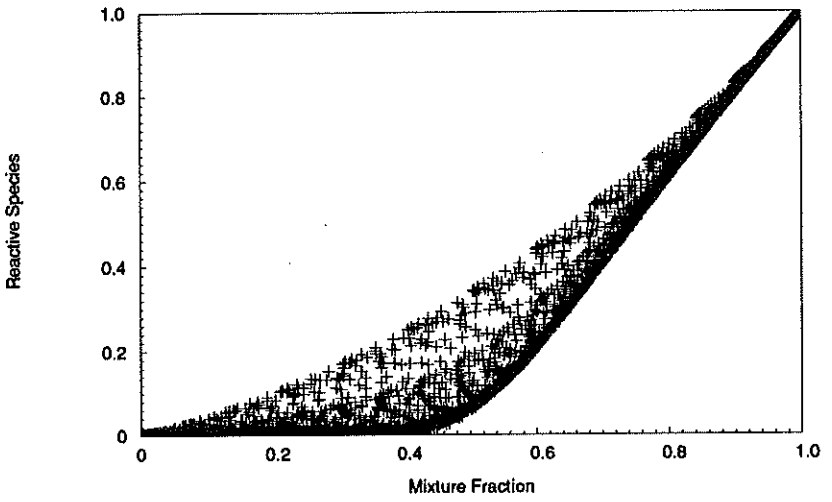

FIGURE 1. Distribution of the reactive species Y_A versus mixture fraction Z.

($\chi = 2\mathcal{D}|\nabla Z|^2$), is found to be well correlated with the tangential strain rate evaluated at the flame surface. Gibson's theory for constant density flows (Gibson 1968) predicts a value of -0.5 for the correlation coefficient between strain rate and scalar dissipation rate. Incompressible DNS (Nomural *et al.* 1992) report values ranging from -0.4 to -0.5. The present simulations provide a value of -0.6. This larger value is likely to be a result of dilatation associated with heat release in our computations. As expected, the scalar gradient is also found to be most probably aligned with the most compressive strain rate direction.

In accord with laminar flamelet theory (Peters 1986), the scalar dissipation rate increases with reaction rate until a critical value is reached at which extinction occurs. Early in the simulation (i.e. within one eddy turnover time), the maximum value of the reaction rate interpolated along the local flame surface normal vector and plotted versus the scalar dissipation rate follows the common laminar flamelet response, Figure 2. However, when the flame is undergoing "full interaction" with turbulence, see Figure 3, a deviation from the bounds indicated by laminar flamelet is observed and is related to the transient effects observed in Figure 1.

The reason for this deviation is due to the reaction rate being influenced by the local temperature but also by the species mass fraction. It appears that turbulent-enhanced mixing convects more species to the reaction zone than in a pure strained laminar flamelet. The vorticity does not penetrate the flame except at locations where extinction is observed. Indeed, within the flame region, the dynamic viscosity increases with temperature, creating a zone of large dissipation which has the effect of damping the turbulence. These observations suggest that even if the fluid mechanics features of the flow are close to the flamelet regime the dynamic information carried by the turbulence introduces some transient effects that certainly need to be included in the modeling to predict the mean burning rate capturing

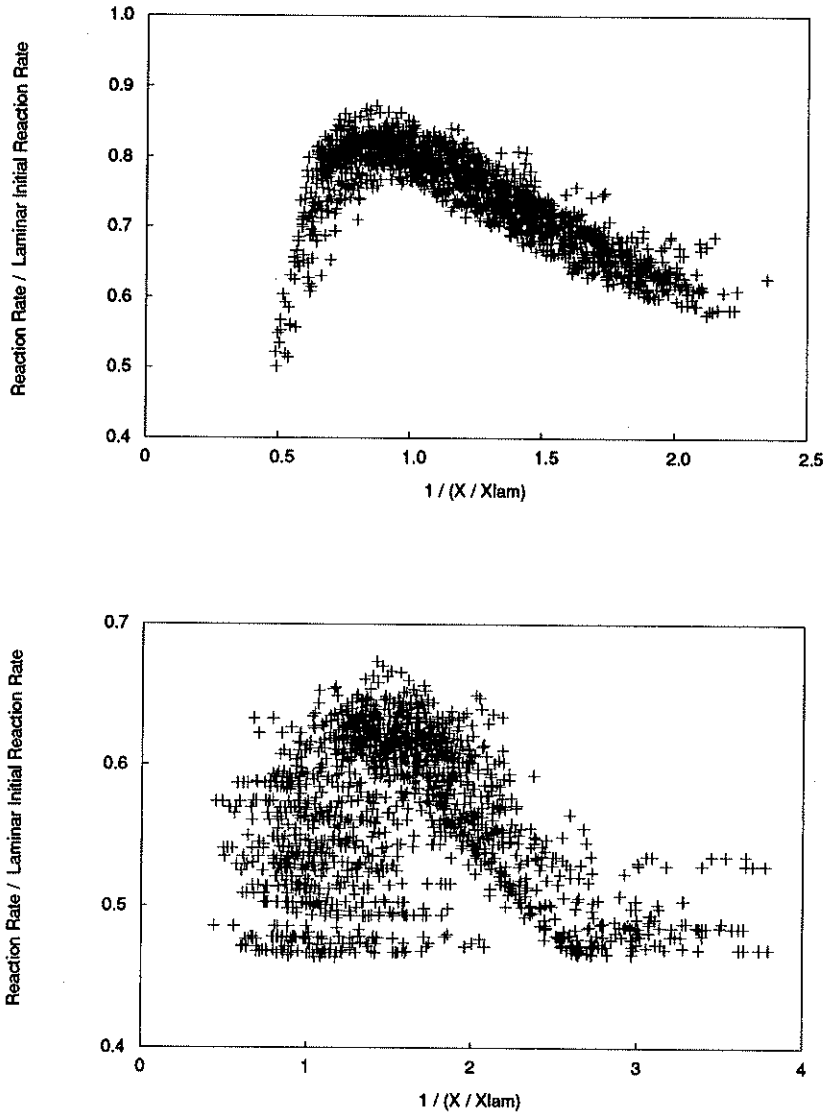

FIGURE 2 AND 3. Distribution of the maximum reaction rate with respect to the inverse scalar dissipation rate $1/(\chi/\chi_{lam})$, for two successive times.

with accuracy finite-rate chemistry effects.

The pdf modeling shifts the problem of the evaluation of the mean burning rate to the estimation of the small scale mixing (Dopazo 1992). Hence, this approach is promising when the mixing process is not too much influenced by the reaction, allowing the chemical kinetics to decouple from the fluid dynamics. The distribution of the reactive species dissipation rate χ_{Y_A} ($\chi_{Y_A} = 2\mathcal{D}_A|\nabla Y_A|^2$) is a quantity representative of the intensity of mixing and is found in the simulations to be

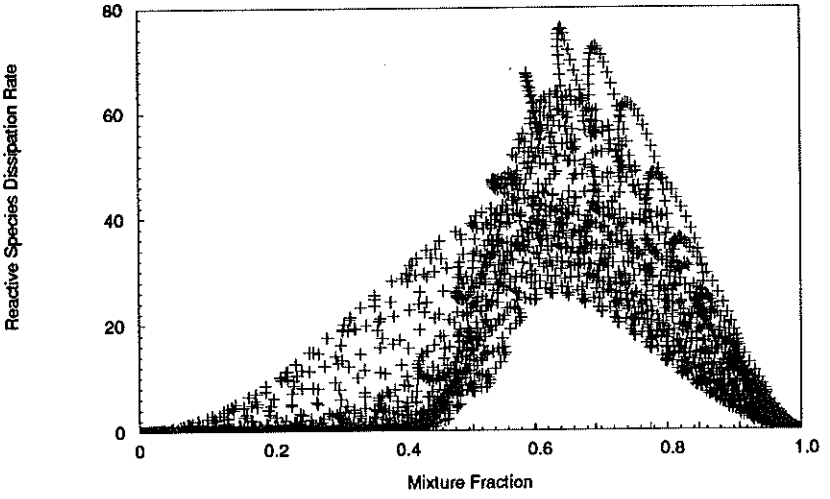

FIGURE 4. Distribution of the reactive species A dissipation rate with respect to the mixture fraction Z, slow chemistry.

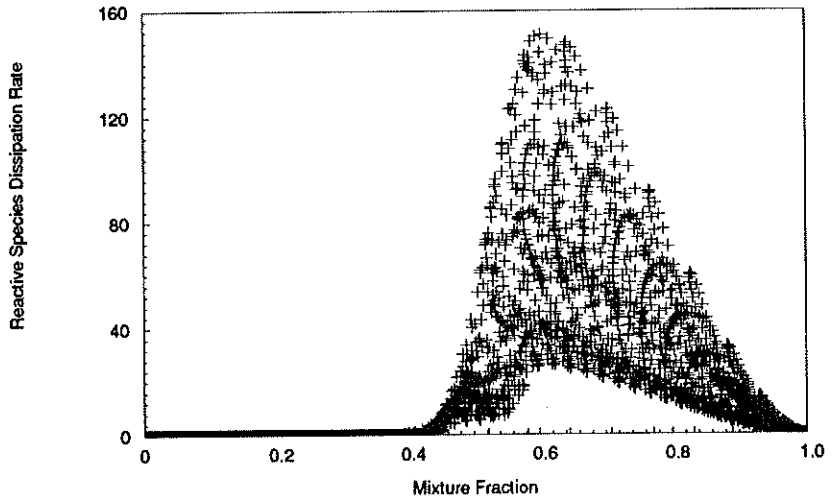

FIGURE 5. Distribution of the reactive species A dissipation rate with respect to the mixture fraction Z, fast chemistry.

sensitive to the Damköhler number. Actually, in the limit of very fast chemistry, the properties of the small scales of the reactives species field are known to be more sensitive to the chemical reaction than to the turbulent cascade energy process (Kuznetsov *et al.* 1990, p61). Thus it is hardly surprising that the reactive effect can still be perceived for intermediate values of the Damköhler number.

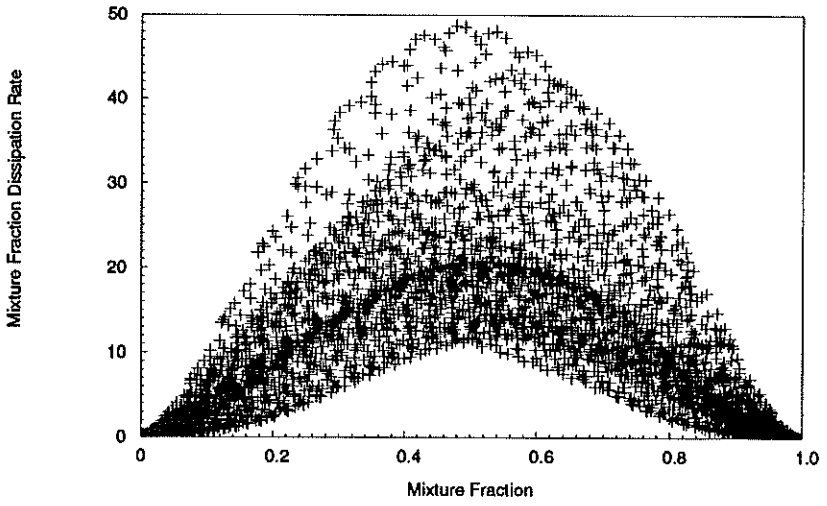

FIGURE 6. Distribution of the mixture fraction dissipation rate χ versus mixture fraction, slow chemistry.

In Figure 4, two zones are observed, corresponding to Figure 1 or Figure 3. When the Damköhler number is large, Figure 5, the dissipation rate is negligible for $Z < 0.4$, whereas for the slower chemistry, Figure 4, a finite bound appears. This figure displays the penetration of the species A in the other side of the flame, creating, at the very least, a partially premixed situation. Here, the same physical turbulent-induced processes are observed than those previously noticed in the investigation of the local flame topology. Locally, the gradient of the reactive species are simultaneously influenced by both reaction rate and turbulent transports. Therefore, even in non-premixed combustion, it is difficult to conclude that small scale mixing is unaffected by the reactive processes.

Consequently, the estimation of a mean mixing time scale (used in any mixing model) without including information related to the reactive activity can lead to large disagreement between numerical predictions and measurements since the fluid dynamics motion is then somewhat disconnected from the kinetics (Chen *et al.* 1990, Borghi *et al.* 1990). A way to overcome this deficiency could be the introduction in the modeling of informations related to the gradient of the species field (Fox 1992a, Mantel *et al.* 1990).

The same approach is used to study the sensitivity of the mixture fraction dissipation rate χ to finite-rate chemistry and turbulence-induced transient effects connected with those mentioned above. A detailed comparison of reactive and non-reactive fields indicates that the distribution of the mixture fraction dissipation rate is sensitive to the chemical processes. This is attributed directly to the modification in density and dynamic viscosity as a result of heat release.

The distribution of the mixture fraction dissipation rate χ appears to lie within an envelope that at first sight follows the response of a typical laminar-like flamelet,

Figure 6. This has also been observed by Fox (Fox 1992b) in the study of the layer-like lamellar system. Usually, it is assumed for modeling purposes that the mixture fraction and its dissipation rate are uncorrelated quantities (Kuznetsov 1990 p60, Peters 1986, Warnartz *et al.* 1986). Figure 6 indicates that the turbulence randomizes the values but that they are not completely uncorrelated.

2.2 Two-step chemistry model

The structure of the reaction zone obtained with the two-step chemistry in the case of slow chemistry is more complex. The intermediate species, I, field is such that a production-recombination zone lies on the oxidizer side of the domain ($Z < 0.5$), and a diffusion zone is observed on the fuel side, Figure 7. If the second reaction was suppressed, the dissipation rate of the intermediate species χ_{Y_I} ($\chi_{Y_I} = 2\mathcal{D}_I \mid \nabla Y_I \mid^2$) would present two symmetric peaks on either side of the value $Z = 0.5$ with a minimum at this point. Since I is consumed by A in the second reaction step, the maximum value of the dissipation rate is enhanced relatively to the peak on the B side, with a minimum shifted to approximately $Z = 0.4$ (location of the generation of I by the first step), Figure 8.

The two reaction zones are not completely segregated in physical and mixture fraction space. However, for the same value of the Damköhler number, the global contribution of the reaction to the energy source term is broader in mixture fraction space than the corresponding contribution in the case of one-step chemistry. This event makes the flame less susceptible to undergoing local extinction compared to a flame modeled with single-step. This suggests that the modeling of extinction is strongly connected to the choice of the chemical scheme in terms of number of steps and species involved.

3. Unequal diffusivity effects in non-premixed flames

Within hydrogen or hydrocarbon flames, mono-atomic hydrogen and diatomic hydrogen atoms are present with heavier species that diffuse more slowly. The laminar flame structure is known to be strongly dependent on the larger diffusivity of radical species, which plays an important role in the ignition processes. One way to determine if, despite the large turbulent-induced transports, unequal diffusivity effects persist in turbulent non–premixed flames is to compare, from experimental results, the value of mixture fraction based on hydrogen atom with those based on carbon atom. Vranos (Vranos *et al.* 1992) investigated Methane-Hydrogen flames at high Reynolds numbers and reported differences between the two different mixture fractions, indicating that unequal diffusivities effects are present.

In most of the turbulent non-premixed combustion models, the hypothesis that all the species diffuse at the same rate is used. Thus the analysis of DNS databases including Schmidt number effects in non–reacting and in reacting flow is relevant.

3.1 Unequal diffusivity effects in non–reacting flows

To investigate the effect of varying the Schmidt number on the small scale mixing, first DNS of non–reacting flows have been carried out.

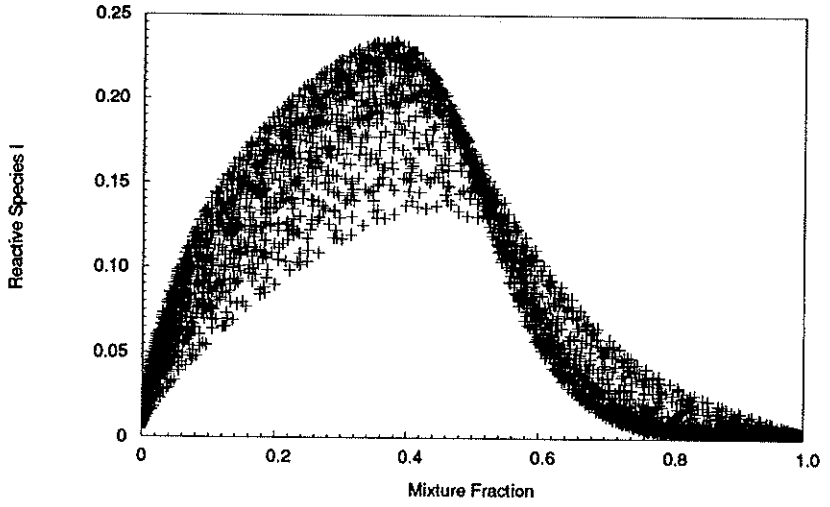

FIGURE 7. Distribution of the intermediate reactive species I versus mixture fraction, slow chemistry.

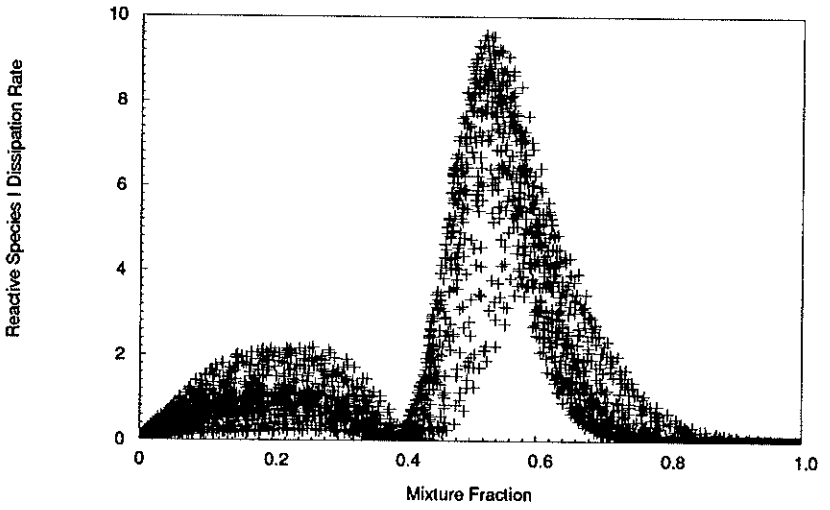

FIGURE 8. Distribution of the dissipation rate of the intermediate reactive species I versus mixture fraction, slow chemistry.

In the free decaying turbulence configuration, a species C is added on the "A-side" with a Schmidt number equal to one-half. The laminar initial pure diffusive zone is then allowed to interact with the turbulence. If the scatter plot of Y_C versus Y_A does not show the evidence of differential diffusion effect as in the experiment of Smith (Smith *et al.* 1992), the distribution of the ratio $r_1 = \frac{Y_A}{Y_C}$, Figure 9, clearly

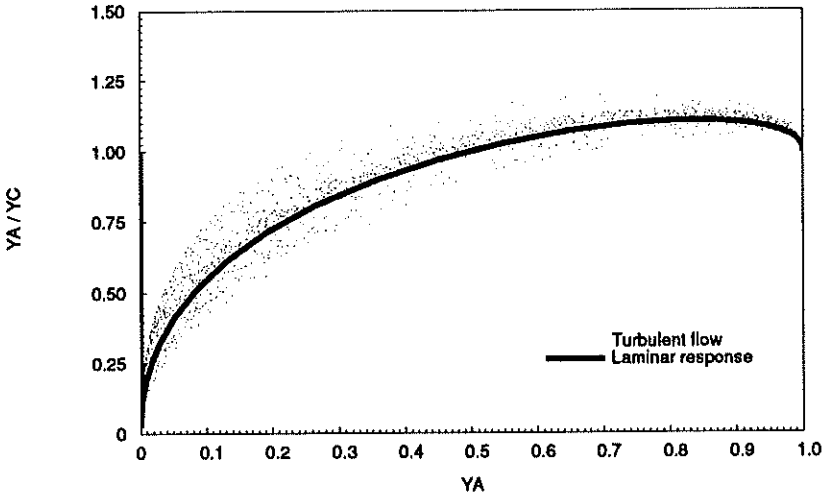

FIGURE 9. Distribution of the ratio $r_1 = \frac{Y_A}{Y_C}$ versus Y_A; pure mixing situation.

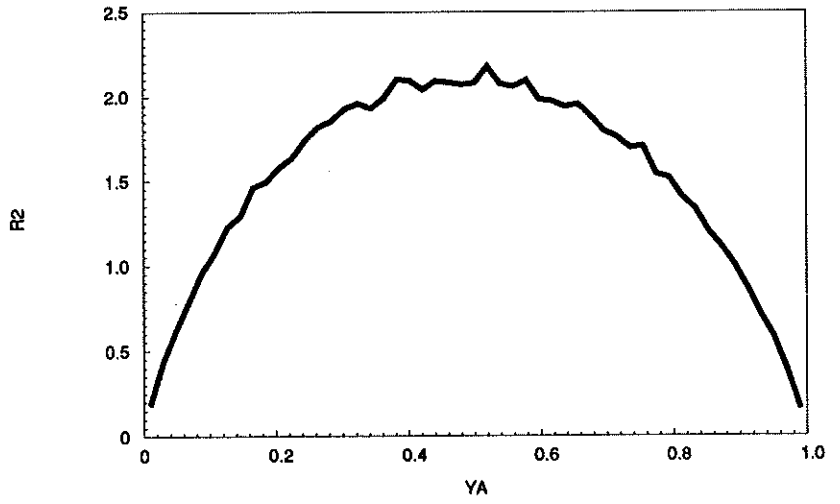

FIGURE 10. Ratio $r_2 = \frac{\langle |\nabla Y_A|^2 | Y_A = \Psi_A \rangle}{\langle |\nabla Y_C|^2 | Y_A = \Psi_A \rangle}$ versus Y_A; pure mixing situation.

demonstrates the presence of this differential diffusion effects. Figure 9 displays for the same time the laminar equivalent evolution (where the exact solution is known) and the scatter plots of r_1 corresponding to the turbulent flow (the equal diffusivity problem would provide $r_1 = 1$). The turbulence induces a spreading of the points around the laminar response, and when Y_A tends to zero, the ratio r_1 also tends to zero. Both of these observations reveal that small scale diffusion is sensitive to the

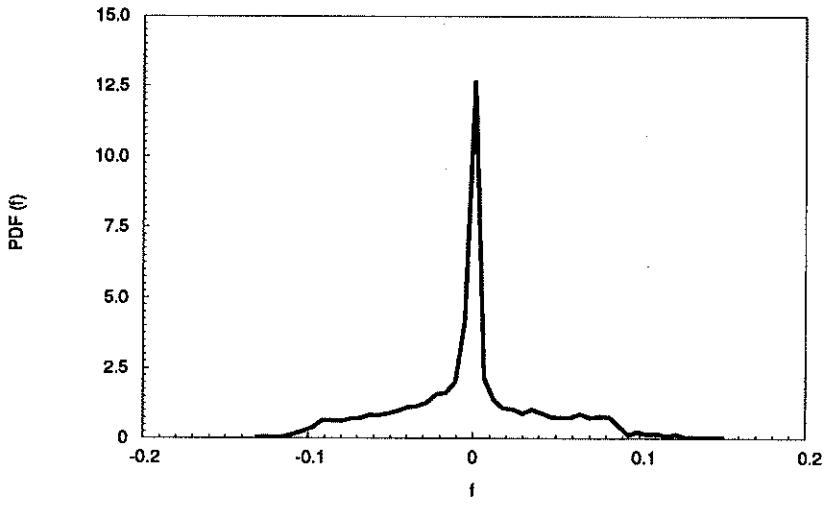

FIGURE 11. pdf of the differential diffusion variable; pure mixing situation.

smaller Schmidt number of the species C. The ratio of the conditional mean values for the magnitude of the gradient of the species A and C, $r_2 = \frac{\langle |\nabla Y_A|^2 | Y_A = \Psi_A \rangle}{\langle |\nabla Y_C|^2 | Y_A = \Psi_A \rangle}$, is presented in Figure 10. This quantity reaches its maximum when $Y_A = 0.5$ and its minimum at the edge of the composition space, with large variations around the value $r_2 = 1$ corresponding to equal diffusivity. Kerstein (Kerstein 1990) proposed to define a differential diffusion variable, f, as: $f = Y_A - Y_C$. The pdf of this quantity is proposed in Figure 11. This pdf is somewhat symmetric around $f = 0$, with unequal zero value tails. The examination of the three previous quantities demonstrates that differential diffusion effects occur in pure mixing simulations. The turbulence induces a deviation from the laminar diffusive motion, but the unequal diffusive effect can still be perceived.

Increasing the Reynolds number will decrease the scales at which the laminar diffusive process is acting. In large Reynolds number reacting flows, because of significant increase in kinematic viscosity with temperature, the differential diffusion effects pointed out above will certainly still be present at the diffusive scales where chemical activities occur, especially for very fast diffusive radical species.

3.2 Unequal diffusivity effects in reacting flows

If the Schmidt number of all the species is assigned a value of unity, the pdf of the curvature of the three dimensional flame is found to be symmetric (the surface exhibits both positive and negative curvature). However, when the Schmidt number of the species A is changed to one half (one-step chemistry) the probability of negative curvature along the stoichiometric surface increases, Figure 12. Negative curvature in this instance corresponds to reaction zones that are curved into the "B-side". This observation is correlated with the broader reaction zone found on

this side in mixture fraction and physical space. The same trend has been found by Trouvé (Trouvé 1991) in the case of premixed combustion.

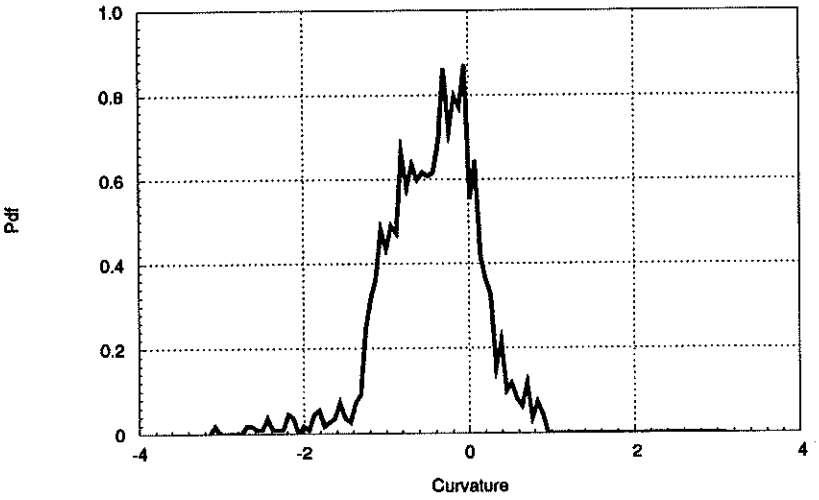

FIGURE 12. Pdf of the curvature along the flame surface; fast chemistry.

In the two-step chemistry case without changing the initial turbulent field but modifying the Schmidt number of the intermediate species, I, DNS allows us to study the impact on the flame of a fast diffusive radical-like species. The contour plots of the intermediate species dissipation rate presents two areas related to the production-consumption and pure diffusion zones of I. For $Sc_{Y_I} = 0.5$, the two zones are wider than for $Sc_{Y_I} = 1$, Figure 13. This observation is related to the penetration of the rapidly diffusing intermediate species into both sides of the flame, which modified the magnitude of the dissipation rate but also the shape of the joint pdf of the dissipation rate and mixture fraction (compare Figure 8 and 14).

These results suggest that globally small scale mixing is sensitive to the fast diffusive intermediate species, even though turbulent diffusion is the more active process in term of mean statistical description of the reactive flow field. Further examination of the non-premixed flame response to the unequal diffusivity effects are in progress.

4. Modeling of non-premixed flames

4.1 Introduction

Usually, in industrial computer codes, transport equations for mean quantities (mean mass fraction, mean velocity and mean energy) are solved with the help of classical turbulence models for the Reynolds stress and the turbulent flux (usually Favre averaging is chosen, $\overline{A} = \frac{\langle A\rho \rangle}{\langle \rho \rangle}$). The validity of these turbulence models in the case of reacting flows with variable density will not be discussed here. The

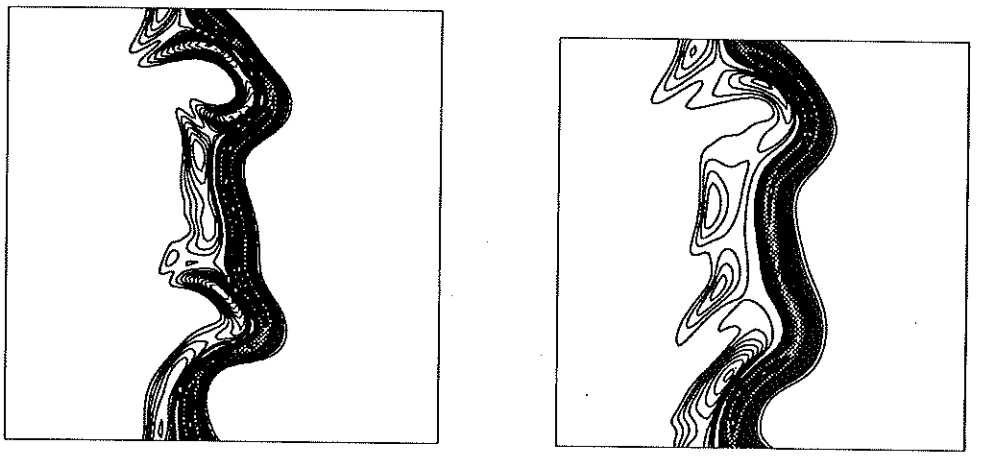

FIGURE 13. Intermediate species dissipation rate contours, on the left $Sc_I = 1$, on the right $Sc_I = 0.5$.

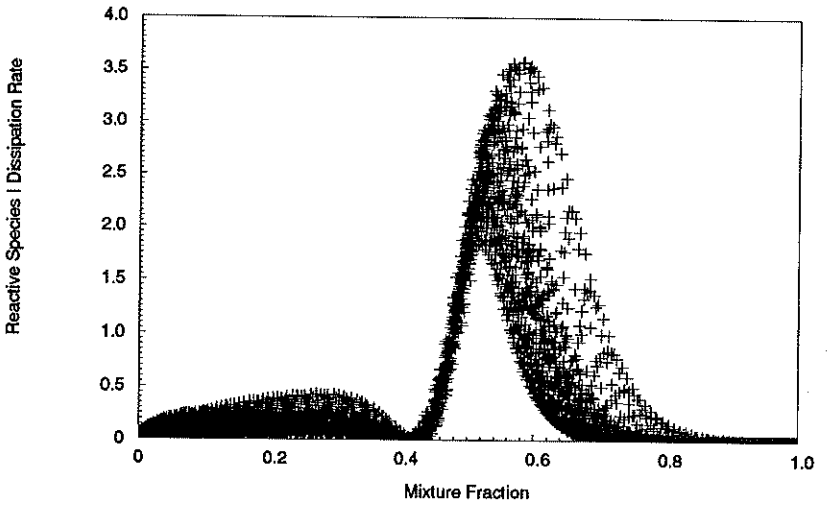

FIGURE 14. Distribution of dissipation rate of intermediate species I versus mixture fraction; $Sc_I = 0.5$.

mean reaction rate that appears in the mean species transport equation needs to be modeled and the aim of the method proposed in the following is to built a kind of "pdf generator" which generates, at a low cost, an approximated pdf of the thermochemical variables. This is with enough accuracy to compute in non-premixed flame in air the mean reaction rate of the oxidizer, $\overline{\dot{\omega}}_{Ox}$.

The chemistry is described through one global reaction step and heat losses by

radiative transfer are neglected; therefore, two variables (mixture fraction and oxidizer mass fraction) only are required for the description of the reactive flow field. This is a very crude approximation, but for engineering purposes, instead of using the local equilibrium hypothesis, it is useful to compute a first approximation of the reactive flow field which accounts for the interaction between the turbulent and chemical processes. This approximation can then be used to study the behavior of global parameters or to initialize more precise and more time consuming computer methods, such as Monte Carlo Methods able to deal with complex chemistry (Jones *et al.* 1985).

The DNS results of turbulent non-premixed flames discussed previously indicate that transient effects have to be included in the modeling. Especially, the scatter plots of the reactive scalar concentration, temperature, and reaction rate show that the pdf of the reactive species exhibits a continuous shape between the frozen flow line and the equilibrium line.

Two curves $y^1_{Ox} = y^1_{Ox}(Z)$ and $y^2_{Ox} = y^2_{Ox}(Z)$ clearly limit the spreading of the pdf in the plane (Y_{Ox}, Z), $(y^1_{Ox} \leq y^2_{Ox} \quad \forall\ Z)$. The mean burning rate can be computed from an estimated pdf $\overline{P}(Y_{Ox}, Z)$ supported by an area located between y^1_{Ox} and y^2_{Ox}. Three pieces of information are needed to perform this evaluation, the approximated location of the pdf in the concentration space, the extend of spreading, and the local amplitude of the pdf. The location of the pdf and the control on the extend of spreading will be based on the simplified probability density function approach (Borghi *et al.* 1983, Gonzalez *et al.* 1986). A way to evaluate the local amplitude of the pdf is derived from the DNS observations.

4.2 A new formulation for the presumed pdf method

Using information issued from the mean flow field, Borghi (Borghi *et al.* 1983) first proposed to built an approximation of $\overline{P}(Y_{Ox}, Z)$. This approximated pdf was obtained with the help of the Dopazo (Dopazo *et al.* 1976) small scale mixing model (also call *iem* Lagrangian model) and possessed some of the characteristics of the mean reactive scalar field. This model included some properties of the conditional pdf $\overline{P_c}(Y_{Ox}|Z)$, $\left(\overline{P_c}(Y_{Ox}|Z) = \frac{\overline{P}(Y_{Ox},Z)}{\overline{P}(Z)}\right)$, where $\overline{P}(Z)$ was presumed as a Beta function with the two parameters $\overline{Z}$ and $\overline{Z'^2}$.

Inside a two-inlet homogeneous reactor, when the pdf is discretized with two particles (one for each inlet), the evolution of the particles concentration equivalent to the pdf transport equation closed with the *iem* mixing model is (Pope 1979):

$$\frac{dy_{Ox}}{dZ} = \frac{\dot{\omega}_{Ox}\tau_{t_{Ox}} + \overline{Y}_{Ox} - y_{Ox}}{\overline{Z} - Z}. \tag{2}$$

The quantity $\tau_{t_{Ox}}$ is a mixing time scale, and when only mean values are known, the previous equation is a closed form of Eq.(1). According to DNS observations, a transport equation must be solved for the mean dissipation rate of the reactive species $\overline{\varepsilon}_{Y_{Ox}}$ and also for the rms of the reactive species $\overline{Y'^{\,2}_{Ox}}$ to get $\tau_{t_{Ox}} = \frac{\overline{Y'^{\,2}_{Ox}}}{\overline{\varepsilon}_{Y_{Ox}}}$.

This estimation of $\tau_{t_{Ox}}$ allows the inclusion of information coming from the reactive processes into the mixing model.

The homogeneous situation related pdf, $\overline{P_c}(Y_{Ox}|Z)$, can be written:

$$\overline{P_c}(Y_{Ox}|Z) = \delta\left(y_{Ox}^{iem}(Z) - Y_{ox}\right), \tag{3}$$

where $y_{Ox}^{iem}(Z)$ is composed of two trajectories obtained by solving (2) with the boundary conditions: $(y_{Ox} = 0, Z = 1)$ and $(y_{Ox} = 1, Z = 0)$.

In non homogeneous flows, the shape of the conditional pdf, $\overline{P_c}(Y_{Ox}|Z)$, spreads out, and Borghi (Borghi *et al.* 1983) proposed a way to approximate this pdf in premixed flames. This method has also been extended to non-premixed flame (Vervisch 1992). The pdf, presumed with the help of these previous formulations, reproduced only the mean value of the reactive flow field and was obtained in a discontinuous form, including large holes in the concentration space; moreover, the amplitude of the reactive species pdf was deduced from the amplitude of the mixture fraction pdf. These features are in disagreement with measurements (Masri 1988, Cheng 1991) and previous observations from DNS. An attempt to improve these presumed pdf models is now proposed.

In the DNS field, if the conditional pdf $\overline{P}_c(Y_{Ox}|Z)$ effectively depends on Z, the pdf $\overline{P}_c(\xi|Z)$ where $\xi = \frac{Y_{Ox} - y_{Ox}^1}{y_{Ox}^2 - y_{Ox}^1}$ is only weakly dependent on Z, (Figure 15).

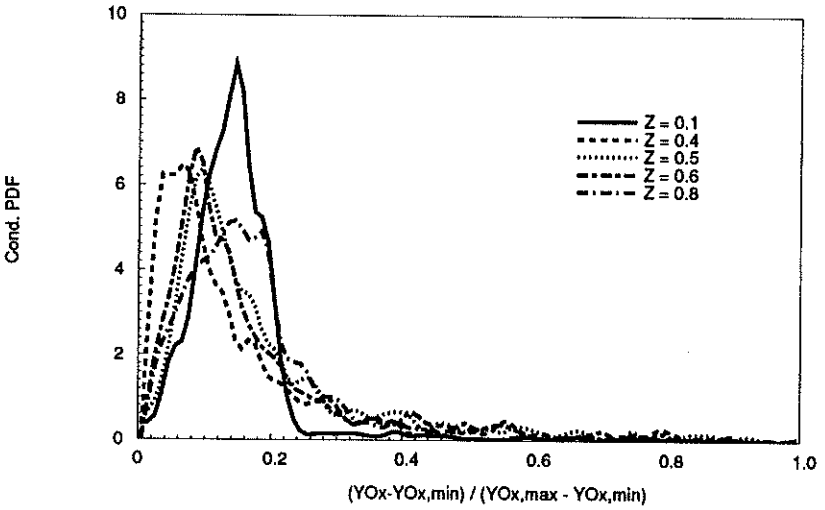

FIGURE 15. Conditional pdf $\overline{P}_c(\xi|Z)$.

Therefore, in the plane (Y_{Ox}, Z), each line between y_{Ox}^1 and y_{Ox}^2, for a fixed value of Z, can be weighted with a reference pdf, $f(\xi)$. The function f, able to mimic situations ranging from low spreading (low oxidizer fluctuations) to the bimodal form (large oxidizer fluctuations), has to be defined as:

$$\begin{gathered}\overline{P}_c(Y_{Ox}|Z) = 0 \quad \text{if } Y_{Ox} < y^1_{Ox}(Z) \text{ or } Y_{Ox} > y^2_{Ox}(Z) \\ \overline{P}_c(Y_{Ox}|Z)\, dY_{ox} = f(\xi)\, d\xi \\ \int_{y^1_{Ox}(Z)}^{y^2_{Ox}(Z)} \overline{P}_c(Y_{Ox}|Z)\, dY_{Ox} = \int_0^1 f(\xi)\, d\xi = 1 \quad \forall\, Z\ .\end{gathered} \tag{4}$$

The estimation of the position of the pdf in the oxidizer mixture fraction plane is achieved when the curve $y^1_{Ox}(Z)$ and $y^2_{Ox}(Z)$ are known. The *iem* trajectory (which contains information on the joint effect of small-scale mixing and reaction) is taken as a reference. The quantity $\overline{y^{iem}_{Ox}} = \int_0^1 y^{iem}_{Ox}(Z)\overline{P}(Z)\, dZ$ is computed. The following possibilities may be considered to determine the curves $y^1_{Ox}(Z)$ and $y^2_{Ox}(Z)$ (Borghi *et al.* 1983):

	$y^1_{Ox} = y^1_{Ox}(Z)$	$y^2_{Ox} = y^2_{Ox}(Z)$
$\overline{y^{iem}_{Ox}} > \overline{Y}_{Ox}$	Equilibrium Line ($\tau_{t_{Ox}} \to \infty$)	*iem* Line
$\overline{y^{iem}_{Ox}} < \overline{Y}_{Ox}$	*iem* Line	Mixing Line ($\tau_{t_{Ox}} \to 0$)

The estimated boundaries being determined, if $f(\xi)$ is a normalized Beta function, $f(\xi) = \frac{\xi^{m-1}(1-\xi)^{n-1}}{\int_0^1 \phi^{m-1}(1-\phi)^{n-1}\, d\phi}$, then the constraints,

$$\begin{aligned}\overline{Y}_{Ox} &= \int_0^1 \int_0^1 Y_{Ox}\overline{P}(Y_{Ox}, Z)\, dY_{Ox}\, dZ \\ &= \int_0^1 \left(\int_{y^1_{Ox}(Z)}^{y^2_{Ox}(Z)} Y_{Ox}\overline{P}_c(Y_{Ox}|Z)\, dY_{Ox} \right) \overline{P}(Z)\, dZ \\ \overline{Y'^{\,2}_{Ox}} &= \int_0^1 \int_0^1 (Y_{Ox} - \overline{Y}_{Ox})^2 \overline{P}(Y_{Ox}, Z)\, dY_{Ox}\, dZ \\ &= \int_0^1 \left(\int_{y^1_{Ox}(Z)}^{y^2_{Ox}(Z)} (Y_{Ox} - \overline{Y}_{Ox})^2 \overline{P}_c(Y_{Ox}|Z)\, dY_{Ox} \right) \overline{P}(Z)\, dZ\ ,\end{aligned} \tag{5}$$

according to the properties of the β function, lead to:

$$\begin{aligned} n &= \frac{(\Omega_1 - 1)(1 - \Omega_2)}{(1 - \Omega_2)\Omega_1 - \Omega_2(1 - \Omega_1)} \\ m &= \frac{\Omega_1(\Omega_2 - 1)}{(1 - \Omega_2)\Omega_1 - \Omega_2(1 - \Omega_1)}\ , \end{aligned} \tag{6}$$

where :

$$\Omega_1 = \frac{\overline{Y}_{Ox} - \overline{y^1}_{Ox}}{\overline{y^2}_{Ox} - \overline{y^1}_{Ox}}$$

$$\Omega_2 = \frac{\overline{Y'^2_{Ox}} - 2\left(\overline{y^1_{Ox}(y^2_{Ox} - y^1_{Ox})} - (\overline{y^2}_{Ox} - \overline{y^1}_{Ox})\overline{Y}_{Ox}\right)\Omega_1}{\overline{(y^2_{Ox} - y^1_{Ox})^2}\Omega_1} \qquad (7)$$

$$- \frac{\left(\overline{(y^1_{Ox})^2} - 2\overline{y^1}_{Ox}\overline{Y}_{Ox} + \overline{Y}^2_{Ox}\right)}{\overline{(y^2_{Ox} - y^1_{Ox})^2}\Omega_1} .$$

(In the equations, the mean values are defined as: $\overline{a} = \int_0^1 a(Z)\overline{P}(Z)\,dZ$.)

The mean reaction rate $\overline{\dot{\omega}}_{Ox}$ can then be computed to advance the equation in time in the Navier Stokes solver,

$$\begin{aligned}\overline{\dot{\omega}}_{Ox} &= \int_0^1 \int_0^1 \dot{\omega}_{Ox}\overline{P}(Y_{Ox}, Z)\,dY_{Ox}\,dZ \\ &= \int_0^1 \left(\int_{y^1_{Ox}(Z)}^{y^2_{Ox}(Z)} \dot{\omega}_{Ox}\overline{P}_c(Y_{Ox}|Z)\,dY_{Ox} \right) \overline{P}(Z)\,dZ\ .\end{aligned} \qquad (8)$$

this is performed until the steady state is reached.

This dynamic "pdf generator" is able to follow different shapes of pdf according to the level of turbulence (through the quantities, $\overline{Z}$, $\overline{Z'^2}$, $\overline{Y}_{Ox}$, $\overline{Y_{Ox}'^2}$, $\tau_{t_{Ox}}$, chemistry model parameters). The finite rate chemistry effect is implicitly included in the mixing model, especially when the time scale includes informations related to the chemistry. Unlike the previous formulation, the pdf is presumed in a continuous form, reproducing the transient effect observed in the DNS simulations. This simple model can be improved using more elaborate mixing model (Gao 1992) and can be of great interest to initialize the Monte Carlo method to reduce the large amount of computer time.

5. Future plans

The study of the turbulent flame structure modeled with two-step chemistry will be completed introducing a third step, $B + I \rightarrow P$, allowing the species I to undergo recombination on both sides of the flame.

The configuration also needs some improvement; a shear will be included in the simulations using the methodology developed by Trouvé (Trouvé 1992). This is to study a model flow problem with properties closer to the non-premixed jet flame situation.

Acknowledgements

Dr. Arnaud Trouvé and Dr. Feng Gao are thanked for their helpful comments and suggestions. The author also acknowledges his fruitful interaction with Dr. Jacqueline Chen, Prof. Shankar Mahalingam, Prof. Ishwar Puri, and Dr. Poinsot.

REFERENCES

BORGHI, R., VERVISCH, L., & GARRETON, D. 1990 The calculation of local fluctuations in non-premixed turbulent flames. *Eurotherm.* **17,** Oct. 8-10, Cascais.

BORGHI, R., & POURBAIX, E. 1983 Lagrangian models for turbulent reacting flows. *Turbulent Shear Flow conferences No 4* Springer-Verlag.

CHEN, J. H., MAHALINGAM, S., PURI, I. K., & VERVISCH, L. 1992 Effect of finite–rate chemistry and unequal schmidt numbers on turbulent non–premixed flames modeled with single–step chemistry. *Paper WSS/CI 92-52, Western States Section of the Combustion Institute Fall meeting, Berkeley.*

CHEN, J. H., MAHALINGAM, S., PURI, I. K., & VERVISCH, L. 1992 Structure of turbulent non-premixed flames modeled with two-step chemistry. *Paper WSS/CI 92-51, Western States Section of the Combustion Institute Fall meeting, Berkeley.*

CHEN, J. Y., & DIBBLE, R. W. 1990 Application of reduced chemical mechanism for prediction of turbulent non-premixed methane jet flames. Sandia report 90-8447.

CHENG, T. S., WEHRMEYER, J. A., & PITZ, R. W. 1991 Simultaneous temperature and multi-species measurement in a lifted hydrogen diffusion flame by a KrF excimer laser. *AIAA 29th Aerospace Sciences Meeting* January 7-10, Reno, Nevada.

COUPLAN, J., & PRIDDIN, C. H. 1987 Modelling the flow and combustion in a production gas turbine combustor. *Turbulent Shear Flow conferences No 5* Springer-Verlag, Heidelber, August 7-9.

DIBBLE, R. W., SCHEFER, R. W., CHEN, J.-Y., HARTMANN, V., & KOLLMAN, W. 1986 Velocity and density measurements in a turbulent non-premixed flame with comparison to numerical model predictions. *Paper WSS/CI 86-65, Western States Section of the Combustion Institute Spring Meeting, Banff, Canada.*

DOPAZO, C. 1992 Recent developments in pdf methods. *To be published.*

DOPAZO, C., & O'BRIEN, R. 1976 An approach to the autoignition of a turbulent mixture. *Department of Mechanics State University of New York, Stony Brook,* N.Y. 11790.

FOX, R. O. 1992a The Fokker-Plank closure for turbulent molecular mixing. *Physics of fluid.* **A4 (6),** 1230-1244.

FOX, R. O. 1992b On the joint scalar, scalar gradient pdf in lamellar system. *To be published.*

GIBSON, C. H. 1968 Fine structure of scalar fields mixed by turbulence: I. Zero gradient points and minimal gradient surfaces. *Phys. Fluids.* **11,** 2305.

GAO, F. 1992 A mixing model for pdf simulations of turbulent reacting flows. *Annual Research Briefs 1992.* CTR, Stanford U./NASA Ames.

GONZALEZ, M., & BORGHI, R. 1986 Application of Lagrangian models to turbulent combustion. *Comb. and Flame.* **63,** 239-250.

JONES, W. P., & KOLLMANN, W. 1985 Multi-scalar pdf transport equations for turbulent diffusion flames. *Turbulent Shear Flow conferences No 5,* Springer-Verlag, Heidelber, August 7-9.

KERSTEIN, A. 1990 Linear-eddy modelling of turbulent transport. Part 3. Mixing and differential molecular diffusion in round jets. *J. Fluid Mech.* **216,** 411-435.

KUZNETSOV, V. R., & SABEL'NIKOV, V. A. 1990 Turbulence and combustion. Ed. P. A. Libby, Hemisphere Publishing Corporation.

MAGRE, P., & DIBBLE, R. W. 1988 Finite chemical kinetic effects in a subsonic turbulent hydrogen flame. *Combust. Flame.* **73,** 195–206.

MANTEL, T., & BORGHI R. 1991 A new model of premixed wrinkled flame propagation based on a scalar dissipation equation. *13th ICDERS Meeting.*

MASRI, A. R., BILGER, R. W., & DIBBLE, R. W. 1988 Turbulent non-premixed flames of methane near extinction . *Comb. and Flame.* **73,** 261–258.

NOMURA, K. K., & ELGHOBASHI 1992 Mixing characteristics of an inhomogeneous scalar in isotropic and homogeneous sheared turbulence. *Phys. Fluids.* **A4 (3),** March.

PETERS, N. 1986 Laminar flamelet concepts in turbulent combustion. *Twenty-First Symposium (International) on Combustion.* 1231–1250. The Combustion Institute.

POPE, S. B. 1979 The relationship between the probability approach and particle models for reaction in homogeneous turbulence. *Comb. and Flame.* **35,** 41–45.

POINSOT, T. 1989 Direct simulation of turbulent combustion. *Annual Research Briefs 1989.* CTR, Stanford U./NASA Ames.

POINSOT, T., & LELE, S. 1991 Boundary conditions for direct simulations of compressible viscous flows. *J. Comput. Phys.* **101,** No 1, July 92.

POINSOT, T., VEYNANTE, D., & CANDEL, S. 1991 Quenching processes and premixed turbulent combustion diagrams. *J. Fluid Mech.* **228,** 561–606.

SMITH, L., DIBBLE, R., TALBOT, L., BARLOW, R., & CARTER, C. 1992 Laser raman scattering measurements of differential molecular diffusion in nonreacting laminar and turbulent jet flows. *Paper WSS/CI 92-74, Western States Section of the Combustion Institute Fall meeting, Berkeley.*

TROUVE, A. 1991 Simulation of flame-turbulence interaction in premixed combustion. *Annual Research Briefs 1991.* CTR, Stanford U./NASA Ames.

TROUVE, A. 1992 The evolution equation for the flame surface density in premixed turbulent combustion. *Annual Research Briefs 1992.* CTR, Stanford U./NASA Ames.

VERVISCH, L. 1992 Applications of pdf turbulent combustion models to non-premixed flame calculations. Von Karman Inst. Modeling of Combustion and Turbulence, March 9-3.

VIOLLET, P.-L., GABILLARD, M., & MECHITOUA, N. 1990 Modélisation de plasma en écoulement. *Revue de Phys. Appl.* **25**, 843–857.

VRANOS, A., KNIGHT, B. A., PROSCIA, W. M., CHIAPPETTA, L., & SMOOKE, M. D. 1992 Nitric oxide formation and differential diffusion in a turbulent methane-hydrogen diffusion flame. *Twenty–Fourth Symposium (International) on Combustion.* The Combustion Institute.

WARNARTZ, J., & ROGG, B. 1986 Turbulent non premixed combustion in partially premixed flamelets detailed chemistry. *Twenty–First Symposium (International) on Combustion.* 1533-1541. The Combustion Institute.